USE OF BIFURCATION ANALYSIS IN THE DESIGN AND ANALYSIS OF HELICOPTER FLIGHT CONTROL SYSTEMS

Mr Ryan G. Bedford
Dr. Mark H. Lowenberg
Dept. of Aerospace Engineering,
University of Bristol,
Bristol,
United Kingdom

Abstract

Rotorcraft and their associated flight dynamics are highly non-linear systems, especially in extremities of the flight envelope and under certain flight regimes. It is the application of various criteria to linearized models, along with simulation, that provides the conventional tools for helicopter stability and control studies. The linearized model however only portrays the local dynamics of a non-linear model. Through the incorporation of the non-linearities of a rotorcraft such as non-linear aerodynamics, non-linear control system features and inertial coupling, a global picture of the flight dynamics can be obtained.

Dynamical systems theory provides the basis for the continuation and bifurcation method of analysing non-linear systems of ordinary differential equations. It is considered the principal strength of continuation and bifurcation analysis to indicate and give an insight into phenomena that globally affect behaviour of an aircraft model, as the full non-linear model is used in analysis. The combination of simulation with this form of analysis can provide an extremely powerful tool for the study of non-linear aircraft dynamics.

Modern aircraft and rotorcraft are often intrinsically unstable, and flight is only possible due to a stability and control augmentation system (SCAS). This can introduce additional non-linearities, from both mechanical elements and feedback control systems. This paper will introduce open loop bare airframe bifurcation analysis results of a helicopter model representing a generic light utility helicopter, and proceed to show how the analysis can be used to evaluate the effect of including firstly a stability augmentation system (SAS), and finally a proportional plus integral (P+I) control augmentation system (CAS). It will also look at the effect of control system saturation on the continuation and bifurcation analysis results.

Nomenclature

C_T	- rotor thrust coefficient
C_L	- rotor rolling moment coefficient
C_M	- rotor pitching moment coefficient
$\dot{h}_d$	- pilot demanded earth axes height rate, m/s
K_b	- rotor flapping stiffness, Nm/rad
K_q	- pitch angle feedback constant
K_q	- pitch rate feedback constant
K_f	- roll angle feedback constant
K_p	- roll rate feedback constant
K_r	- yaw rate feedback constant
L	- inflow gain matrix
M	- apparent mass matrix
p, q, r	- roll, pitch and yaw rates, rad/s
r_d	- pilot demanded yaw rate, rad/s
Vt	- total velocity, m/s
x	- system state vector
x_0	- initial starting state vector for continuation
a	- fuselage angle of attack, rad
b	- fuselage angle of sideslip, rad
b_0	- rotor blade coning, rad
b_{1s}	- lateral flapping angle, rad
b_{1c}	- longitudinal flapping angle, rad
f	- fuselage bank angle, rad
f_d	- pilot demanded bank angle, rad
l	- continuation parameter
l_i	- main rotor inflow
l_0	- uniform inflow
l_{1s}	- lateral inflow
l_{1c}	- longitudinal inflow
q	- fuselage pitch angle, rad
q_d	- pilot demanded pitch angle, rad
q_0	- main collective pitch angle, rad
q_{1s}	- longitudinal cyclic pitch angle, rad
q_{1c}	- lateral cyclic pitch angle, rad
q_{0T}	- tail collective pitch angle, rad
W	- rotor rotational speed, rad/s
h_0	- pilot collective lever
h_{1s}	- pilot longitudinal cyclic lever
h_{1c}	- pilot lateral cyclic lever
h_{0T}	- pilot pedal position
y	- rotor blade azimuth position, rad
y_f	- cyclic mixing angle, rad
d	- system parameter vector

1. Introduction

Rotorcraft are highly non-linear systems, and therefore exhibit non-linear flight dynamics. The helicopter also exhibits several principal flying quality deficiencies. Dynamical systems theory provides the basis for the continuation and bifurcation method of analysing non-linear systems of ordinary differential equations. There has been limited research into the application of continuation and bifurcation analysis to rotorcraft (Refs. 1-4), although the benefits of the method have been clearly demonstrated when applied to numerous fixed wing aircraft models (Refs. 5-6). All analysis of rotorcraft to date has been applied to a bare airframe rotorcraft model with no control system present.

It is the application of various criteria to linearized models, along with simulation (generation of time histories), that provides the conventional tools for helicopter stability and control studies. Linearized aircraft models can only portray the local dynamics of a non-linear aircraft model. The time histories obtained from simulation depend upon the starting condition of the model, along with the specific parameter changes invoked during the run, and the varying duration of the simulation, and so the time history generated is specific to those conditions. This limits its use in identifying cause and effect for non-linear phenomena and, when used in isolation, can miss vital mechanisms relating to important aircraft dynamics.

Through the incorporation of the non-linearities of an aircraft model, such as non-linear aerodynamics, inertial coupling and non-linear control system features, a global picture of the aircraft dynamics can be obtained. It is considered that the principal strength of continuation and bifurcation analysis is its ability to indicate and give an insight into phenomena that globally affect behaviour of an aircraft model, as the full non-linear representation is used in the analysis. The bifurcation diagrams produced in this process characterise the steady state 'attractors' and 'repellors' that govern the dynamic behaviour. In combination with non-linear simulation, they can form an extremely powerful tool for the study of non-linear aircraft dynamics.

In this paper, bifurcation analysis is firstly performed on 20th order helicopter model, Helilink, representing an open loop bare airframe generic light utility helicopter. This model was supplied by QinetiQ, Bedford. The model was then augmented with two controllers, raising the order of the model to 24. The system equations model the main and tail rotor as an actuator disc, and include the flapping degree of freedom. The rotor inflow representation is via a three-degree of freedom Pitt-Peters dynamic inflow model. Unsteady aerodynamics are neglected.

This paper aims to demonstrate the effectiveness of the bifurcation and continuation method on the design and evaluation of helicopter flight control systems, and present results of closed loop analysis of rotorcraft models, which, to the authors' knowledge, has not previously been undertaken. This work is to be presented in two ways in this paper.

Firstly, bifurcation diagrams of the bare airframe model are presented, which are then compared with results of two further versions of the model, which include different control systems. The flying quality deficiencies unique to the helicopter would be expected to be made visible through the bifurcation diagrams produced, particularly for the bare airframe model version. These include the impurity of the primary response, whereby the response to pilot control is usually a mix of rate and attitude and varies greatly from hover to high-speed flight. Also, the high degree of cross coupling in all axes will be evident (Ref. 11). The natural instability in the hover, and intrinsic instability associated with hingeless rotors, will show itself in bifurcation results also. This will introduce how continuation and bifurcation analysis can be used to compare and evaluate various control system designs, and how the bifurcation results can be used in conjunction with non-linear simulation. A brief example showing how the effect of a controller proportional gain on system states can be shown through bifurcation analysis.

Previous work on the effect of flight control system saturation on handling qualities (Refs. 7-8), where linear analysis criteria were used to analyse this phenomenon has been conducted. The second objective of this paper is to examine the effect of flight control system saturation on the bifurcation diagrams, and how varying the flight control system saturation limit affects the results. This is investigated for two separate flight conditions, each with a different flight control system in use.

The paper is structured as follows. Section 2 outlines the theory behind the bifurcation and continuation methods used. Section 3 briefly describes the Helilink model and equations of motion in more detail. Section 4 then describes results of the analysis, and Section 5 presents the conclusions.

2. Overview of Continuation and Bifurcation Methods

This section briefly describes the methods associated with performing continuation and bifurcation analysis, and discusses their applicability to aircraft models (Refs. 1-3, 9-10).

The basis for the methodology of continuation and bifurcation analysis is dynamical systems theory. This theory is used to study the behaviour of a non-linear dynamic system, which is described by a set of *n* ordinary differential equations as,

$$\dot{x}(t) = f(x(t), d) \quad x(t) \in \Re^n \; d \in \Re^m \quad (1)$$

where *n* corresponds to the number of components of the state vector *x*, and is the order of the system. In a conventional open loop aircraft model, the state vector *x* consists of the eight fuselage motion or attitude variables (*q, f, Vt, a, b, p, q, r*), and the function *f* consists of the standard flight dynamics equations of motion. The dynamic system is usually dependant on a set of *m* inputs, or parameters of the system, in the case of aircraft usually deflection of the aileron, rudder, etc. and in a helicopter model, the rotor pitch inputs. These will have a large effect on determining the state (flight condition) of the system. Equation (1) describes a general dynamic system, where the function *f* is dependent upon the independent variable time; *t*. This type of system is called non-autonomous. The types of systems considered in this paper are autonomous, and the time *t* does not appear in the function *f;* this covers the vast majority of aircraft models.

The first step in continuation and bifurcation analysis is to calculate the simplest motion a dynamical system can describe - steady states (also called equilibrium states or stationary solutions), which are when the aircraft is in equilibrium and all forces and moments balance so that accelerations are zero. These solution branches of the system can be found by forcing all time derivatives to equal zero, and are then found by solving the algebraic equation.

$$f(x, d) = 0 \quad (2)$$

For any one particular combination of the *m* system parameters, it is possible for more than one of any type of steady state to co-exist in a non-linear system for identical parameter values, and this can provide the system with interesting and complex behaviours. For example, in linear analysis, an unstable solution will diverge to infinity, whereas in the non-linear system, due to the possible existence of multiple solutions, the unstable solution may diverge to another solution branch. In these cases the bifurcation diagrams are of great use in determining the post bifurcationary response. However, for a complete understanding of the non-linear behaviour, time histories are required to understand the transient dynamics of the system, as they are not indicated through continuation and bifurcation analysis. It is also highly desirable to determine the regions of attraction of steady states where possible, to provide separation boundaries between multiple solutions. These can aid in analysing the effect of large perturbations to the system, and determining the state that the system will take.

Apart from stable and unstable steady states, several other types of solutions exist for the ordinary differential equations; these include limits cycles (periodic orbits), quasi-periodic orbits and chaotic motions. Limit cycles are defined by:

$$\dot{x}(t) = \dot{x}(t + T_L) = f(x(t), d) \quad x(t) \in \Re^n \; d \in \Re^m \quad (3)$$

where T_L is the period of the cycle.

The Implicit Function Theorem provides the basis for the numerical techniques known as continuation methods, which provides the methodology for tracing out the solution branches of these steady states of the system, as a single free parameter - the continuation parameter (CP or *l)* - is varied, whilst all other parameters are held fixed. The continuation parameter l is chosen to be one of the members of the parameters d If one steady state is known as an initial starting solution x_0, then pseudoarclength continuation solved by linear extrapolation using Newton's method is utilised to approximate a new steady state. The implicit function theorem states that the equations can be solved provided that the Jacobian matrix of the linearized system is not singular, and that the equations have a continuous first derivative, or are smooth and without discontinuities. These continuation methods are used to generate all the stationary and periodic solutions of the system equations, in the desired state-parameter space of interest. The conventional method of displaying the results from continuation and bifurcation analysis is to plot the solution branches to the ordinary differential equations for each state against the continuation parameter l; this is named a one-parameter bifurcation diagram, and for an n^{th} order system there will typically be *n* one-parameter bifurcation diagrams produced. A sample diagram is shown in Figure 1. It is usually desired to display

stability information and the types, if any, of bifurcations that occur along a solution branch on the bifurcation diagram. It is convention for a solid line to denote a stable steady state and a dashed line to denote an unstable steady state.

Using the Hartman-Groβman Theorem, the local stability of a steady state is found by linearizing the set of equations about the steady state and calculating the eigenvalues. The steady state is locally stable if and only if all eigenvalues have a negative real part, and is locally unstable if the real part of any eigenvalue has a positive real part. If a steady state solution x_0 is stable, the response of the system to a small perturbation remains small as time approaches infinity, and steady state x_0 is unstable if a small perturbation causes the solution to deviate from equilibrium as time progresses. The stability and nature of the solutions can change when one or more eigenvalues crosses the imaginary axis as the continuation parameter is varied, and this can lead to a qualitatively different system response in the system dynamics. This change is called a bifurcation, and the point at which the eigenvalue(s) cross the imaginary axis and the qualitative change occurs is referred to as the bifurcation point.

There are many types of bifurcations possible, and each will have a different effect on the aircraft response. By determining what types of eigenvalues have zero real part at the bifurcation, the qualitative change in the response of the aircraft can be predicted. There are several types of bifurcations that can occur when a single eigenvalue crosses the imaginary axis. Bifurcations points having one zero eigenvalue include limit points (folds, turning points), pitchfork and transcritical bifurcations. The most common of these is the limit point, whereby to one side of the bifurcation point on a 1-parameter bifurcation diagram, two equilibria exist, one unstable and one stable, which merge at the bifurcation point. To the other side of the bifurcation point zero equilibria exist. A Hopf bifurcation, which is when a pair of complex conjugates cross the imaginary axis, is another common bifurcation. This leads to the destruction or creation of periodic orbits from a steady state, depending upon the direction of the continuation parameter variation and of the eigenvalue movement. These types of bifurcations are shown in Figure 1, which also shows the definition of the solution stability through line type. The periodic orbit originating at the Hopf point is not shown.

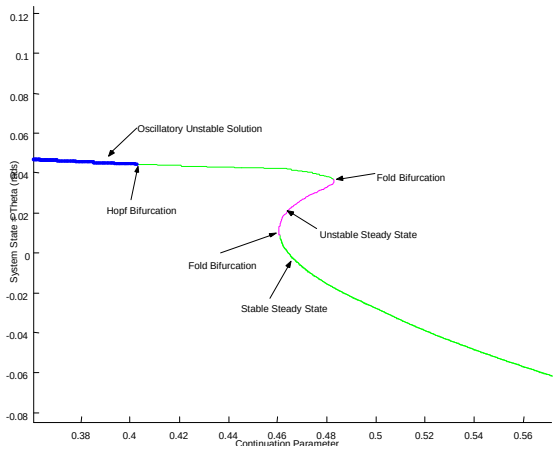

Figure 1. *Sample bifurcation diagram, showing a fold and Hopf bifurcation*

3. Model Description

3.1 Airframe Description The Helilink model utilises rigid body equations of motion for full six degree of freedom flight dynamics, in the form of Eqn. 1. These equations results in an 8th order state vector, Equation (4), which can capture fully the longitudinal and lateral fuselage dynamics.

$$x_f = [q, f, Vt, a, b, p, q, r] \qquad (4)$$

The main rotor and tail rotor systems are modelled as an actuator disc. The main rotor includes the flapping degree of freedom in multi-blade coordinates, with the flapping stiffness modelled as a centrally sprung hinge with stiffness K_b. The main rotor flapping equations can be formulated as a set of second order ordinary differential equations of the form of Eqn. 1, resulting in a state vector of:

$$x_b = \left[b_0, b_{1s}, b_{1c}, \dot{b}_0, \dot{b}_{1s}, \dot{b}_{1c} \right] \qquad (5)$$

A three-degree of freedom Pitt-Peters inflow model of the form of Equation (6) is included, for both the main and tail rotor. This represents rotor inflow up to the first harmonic, as first order coupled linear equations; these add a total of six states to Helilink as in Equation (7).

$$M \begin{Bmatrix} \dot{l}_0 \\ \dot{l}_{1s} \\ \dot{l}_{1c} \end{Bmatrix} + L^{-1} \begin{Bmatrix} l_0 \\ l_{1s} \\ l_{1c} \end{Bmatrix} = \begin{Bmatrix} C_T \\ C_L \\ C_M \end{Bmatrix} \qquad (6)$$

$$x_l = [l_0, l_{1s}, l_{1c}, l_{0T}, l_{1sT}, l_{1cT}] \qquad (7)$$

The thrust, calculated using momentum theory, and blade flapping values calculated from the rotor systems are then transformed

into fuselage axes forces and moments, and applied to the rigid body equations of motion. Pilot control interlinks are also modelled between the pilot's stick and the rotor pitch angles, which essentially counter torque induced rotor moment changes with main collective variation, and so the inputs to the Helilink model are the pilot inceptor positions. This completes the modelling of the bare airframe model upon which initial analysis is performed. The complete state and input vectors are:

$$x=[q, f, Vt, a, b, p, q, r, b_0, b_{1s}, b_{1c}, \dot{b}_0, \dot{b}_{1s}, \dot{b}_{1c}, \ldots\ldots$$
$$\ldots\ldots l_0, l_{1s}, l_{1c}, l_{0T}, l_{1sT}, l_{1cT}]$$
$$d=[h_0, h_{1s}, h_{1c}, h_{0T}] \qquad (8)$$

3.2 Control System Descriptions A simple proportional feedback stability augmentation system (SAS), of partial authority, is then included in the second version of the Helilink model. This is a very straightforward system, which simply comprises constant gain proportional pitch angle and pitch rate feedback to the longitudinal cyclic pitch, proportional roll angle and roll rate feedback to the lateral cyclic pitch, and proportional yaw rate feedback to the pedals. The longitudinal fixed gains were taken from Ref. 11, and all others by approximation from simulation results. A degree of cyclic mixing is also included, with $y_f = 10^o$. The SAS is a limited authority series actuation system, and the rotor pitch actuators are augmented by inputs from the SAS of up to 10% of the full actuator range, after which the controller is saturated. This non-linearity is expected to be evident in bifurcation diagrams produced. The SAS is shown as the inner loop in Figure 2.

The third and final version of the Helilink model considered in this paper contains an attitude command augmentation system (CAS), in addition to the SAS, hence a SCAS. This utilises a proportional plus integral controller on each of the four pilot inceptor channels. Height rate, pitch and roll attitude, and yaw rate are fed back to the pilot collective, longitudinal and lateral cyclic and pedals respectively. The input vector to the Helilink model is now therefore the pilot commanded attitude and rates described above:

$$d=\left[\dot{h}_d, q_d, f_d, r_d\right] \qquad (9)$$

A schematic is shown in Figure 2. The proportional and integral gains are taken from Ref. 12, where the controller described here was designed using eigenstructure assignment for a *Vt*=80kts straight and level flight condition.

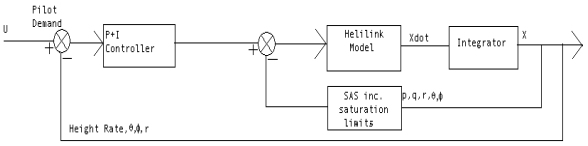

Figure 2. *Block representation of helicopter model FCS*

4. Discussion of Results

4.1 Effects of control systems Bifurcation diagrams are presented in Figure 3 for the bare airframe model, for pitch angle *q*, bank angle *f*, total velocity *Vt,* and angle of attack *a*, with longitudinal cyclic stick h_{1s} as the continuation parameter (CP). Dashed magenta lines indicate asymptotically unstable solutions, blue circles represent 'unstable oscillatory' solutions, and solid green lines stable solutions.

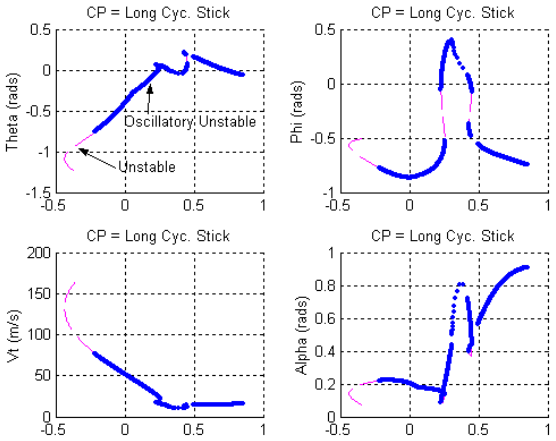

Figure 3. *Bifurcation diagrams of total velocity, pitch angle, bank angle and angle of attack for the bare airframe model. CP=h_{1s}. Starting point is trim at Vt=20m/s*

The starting condition for continuation is straight and level flight at *Vt*=20m/s with h_{1s}=0.191. Throughout continuation all controls are held fixed apart from the CP. The results show that there are no stable solutions present throughout the range of longitudinal stick movement calculated. The large degree of cross coupling is also evident, as in the bifurcation diagram for bank angle *f*, it only remains zero for the initial trim point, and as the CP is varied it rapidly leaves the trimmed value. Now although all solutions found are unstable, the degree of instability and response type is not known, so non-linear simulation is of use to find the actual response. Figure 4 shows the time history for the eight fuselage states, starting from the

Vt=20m/s trim point, with all controls fixed, with h_{1s}=0.191.

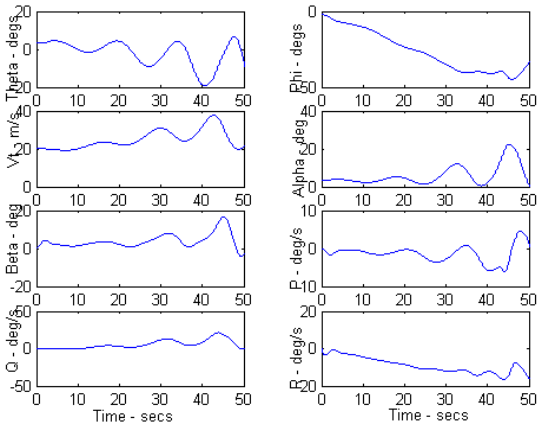

Figure 4. *Simulation Results of bare airframe model, with controls fixed, from straight and level flight at Vt=20m/s*

The simulation results show that indeed the trim solution found is oscillatory unstable as predicted from the bifurcation results. It exhibits a relatively slow divergence and so may be easily controllable by the pilot. Again, significant cross coupling is present, and this divergence is not solely limited to longitudinal states: all lateral states participate in the mode also.

Next, the first closed loop Helilink model with the addition of the SAS outlined in section 3.2 is analysed. Figure 5 shows the bifurcation diagrams with the proportional pitch angle gain K_q as the continuation parameter, with all controls fixed at the *Vt*=20m/s trim values of the bare airframe model which is equivalent to *Vt*≈28m/s with the SAS engaged.

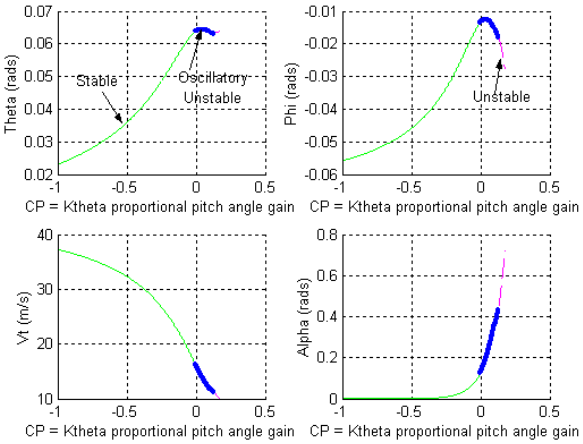

Figure 5. *Bifurcation diagrams of total velocity, pitch angle, bank angle and angle of attack, for Helilink with SAS. CP=K_q. Starting point is trim at Vt≈28m/s*

This can be used as a quick and straightforward way to select a controller gain for stability at a certain flight condition, and examine the effect of the controller gain on the states of the system, but doesn't indicate or guarantee any particular system response. It can be seen that the gain needs to be negative for stability, and as the gain is made more negative, the bank angle also becomes more negative. A value of –0.25 was chosen for K_q.

Figure 6 shows the bifurcation diagrams for *q*, *f*, *Vt*, and *a*, with longitudinal cyclic stick h_{1s} as the continuation parameter CP. Initial parameters and controls correspond to the exact conditions of those for Figure 3 and the bare airframe model.

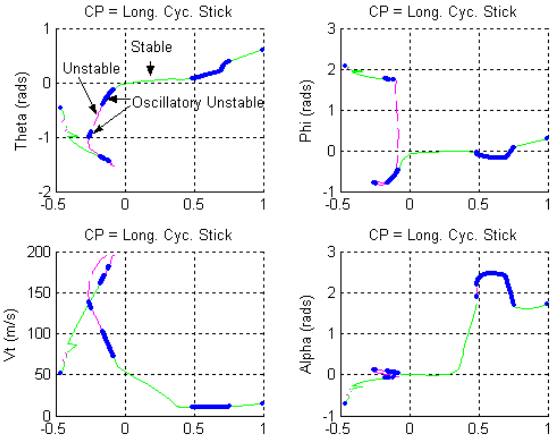

Figure 6. *Bifurcation diagrams of total velocity, pitch angle, bank angle and angle of attack, for Helilink with SAS. CP=h_{1s}. Starting point is trim at Vt≈28m/s*

It is clear that the addition of the simple proportional feedback has stabilised a large region of the solution branch, and between h_{1s}≈-0.1 *and* h_{1s}≈0.4, a conventional trim branch is found, where the helicopter is flying almost straight and level. The quasi-steady response in this region is largely longitudinal only as desired, although off axis response is seen away from this region. It can also be noted that there is a very small change in pitch angle for the large range of total velocity achieved over the conventional trim branch.

As before, non-linear simulation is used to look at the actual response, from a starting condition of a pitch angle of zero degrees. As the solution is now stable, a longitudinal cyclic stick step pitch input of -2^o is applied at *t*=10secs to examine the transient response, and is shown in Figure 7.

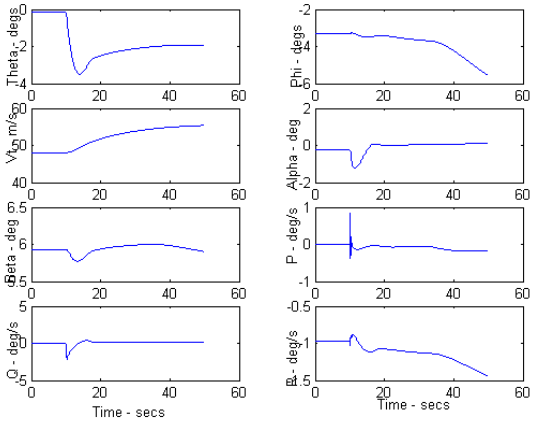

Figure 7. *Simulation Results with controls fixed of Helilink with SAS, from straight and level flight at $q=0^o$*

The flight condition is stable, but the handling is sluggish, with the model taking approximately 15secs to settle to the -2^o pitch angle demanded. There is also off axis response present yet again.

The final version of the model with the SCAS included is now examined. Figure 8 presents the bifurcation diagrams as before. The CP in this case is the pilot demanded pitch angle q_d.

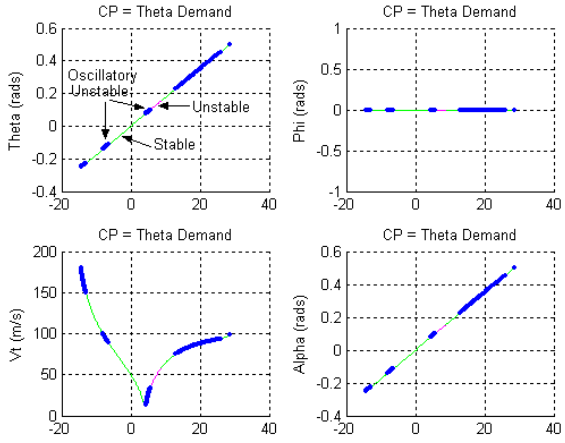

Figure 8. *Bifurcation diagrams of total velocity, pitch angle, bank angle and angle of attack, for Helilink with SCAS. CP=q_d. Starting point is trim at $q_d=0$.*

The stability is largely unchanged from before as is to be expected from the simple addition of a command augmentation system. The bank angle is now zero throughout continuation, showing a perfect longitudinal only response to the longitudinal stick varying, and a linear variation of pitch angle to pitch angle demand. With the addition of the CAS, the pitch angle variation of -6.5^o to 4.5^o for the corresponding demand that describes the conventional trim branch is much larger than with the SAS alone.

The time history for trim at $q_d=0^o$, with a demand input of -2^o at t=10secs is shown in Figure 9.

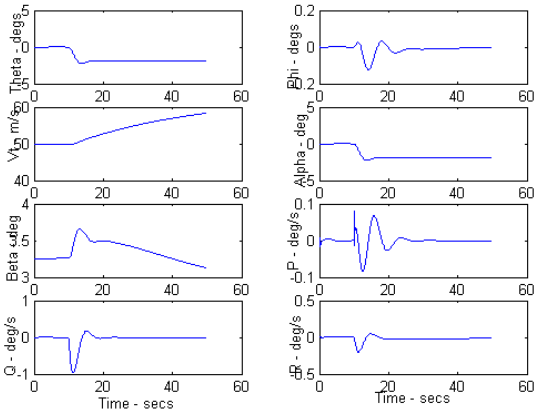

Figure 9. *Simulation Results with controls fixed of Helilink with SCAS, from straight and level flight with $q_d=0$.*

Comparison of this time history with that of Figure 7 shows a much more rapid handling response, with the time taken to approach -2^o pitch angle ~5s. However this is still a little slow. The other most noticeable difference is that the magnitude of the off axis response is much lower and more desirable.

4.2 Control System Saturation In all previous results, the SAS had 10% authority of the full potential rotor pitch, after which it is saturated. The rotor pitch augmentations from the SAS throughout continuation of the Helilink model with only the SAS are shown in Figure 10. They correspond to Figure 6.

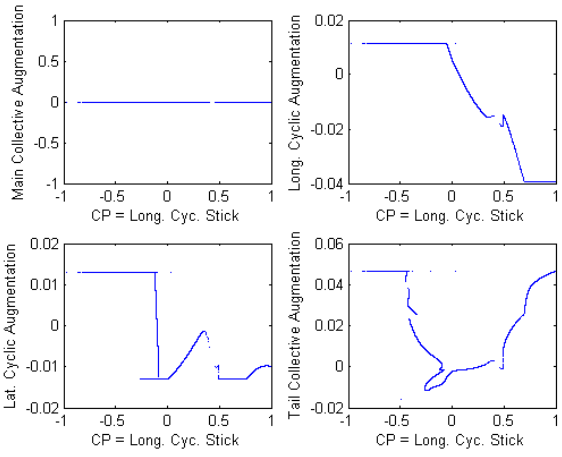

Figure 10. *Rotor augmentations from SAS during continuation of Helilink plus SAS*

The longitudinal cyclic channel saturates at h_{1s}≈-0.05 and h_{1s}≈0.7. It is the saturation at –0.05 that produces the Hopf point and onset of oscillatory unstable solutions at the corresponding CP value in Figure 6. The lateral cyclic channel saturates at h_{1s}≈0.003 and h_{1s}≈0.49. The upper saturation limit

causes the Hopf bifurcation in this case present in the bifurcation diagrams.

The rotor pitch augmentations from the SAS throughout continuation of the Helilink model with the SAS plus CAS are shown in Figure 11. They correspond to the bifurcation diagrams in Figure 8.

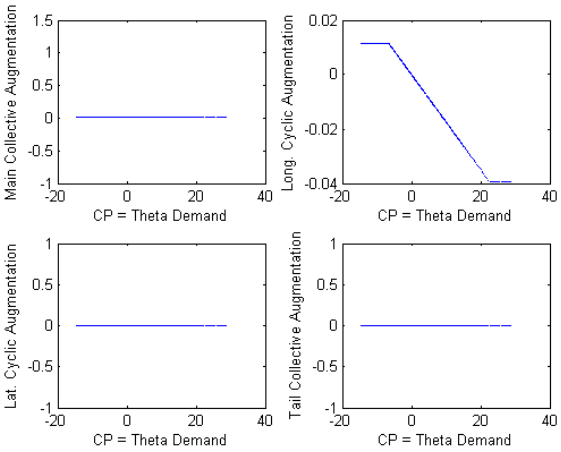

Figure 11. *Rotor augmentations from SAS during continuation of Helilink plus SCAS*

The only augmentation from the SAS in this case is for the longitudinal cyclic pitch. This is due to the fact that all lateral states are held zero by the CAS, hence feedback proportional to these values is also zero. The longitudinal augmentation saturates at $q_d \approx$-6.5° and $q_d \approx$22.5°. A Hopf point coincides with the saturation at $q_d \approx$-6.5°.

The second flight condition to be investigated under the effect of partial authority flight control saturation is a constrained turn, with only the proportional feedback SAS in use. The equations of motion were constrained during continuation to prescribe the turning flight condition. With the constrained states given, the equations for those states could be inverted and solved for the required control values. Longitudinal cyclic is solved such that total velocity is fixed at 50m/s, pedals were solved for sideslip, which is held at zero, and the main collective lever is solved for pitch angle, according to Equation (7), so that it is prescribed in order to define a constrained turn.

$$q = \tan^{-1}[\tan(a)\cos(f) + \tan(b)\sin(f)/\cos(a)] \quad (7)$$

Figure 12 shows a time history of this turning flight condition, with 10% authority assigned to the SAS. As the lateral cyclic stick is moved slowly, quasi statically to port, it shows at a stick position of –0.275 a sudden increase in the rate at which the bank angle is decreasing, which is not desirable.

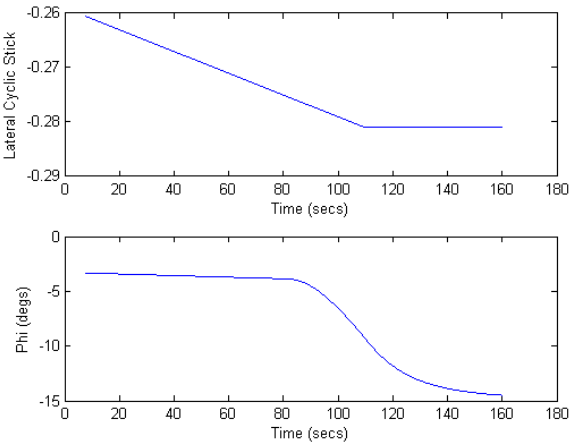

Figure 12. *Time History of turning flight as lateral cyclic stick is moved port, with 10% SAS authority*

Figure 13 shows the bank angle bifurcation diagram where the lateral cyclic stick is used as the continuation parameter, and 10% authority is assigned to the control system (FCS). It shows how at lateral stick values of –0.068 and –0.275, the lateral cyclic FCS augmentation clearly saturates, and the stable flight conditions depart from the lower values of bank angle, and increase suddenly as the lateral stick is moved.

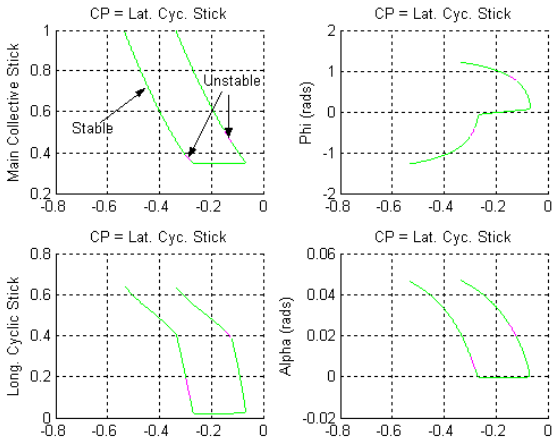

Figure 13. *Bifurcation diagram of bank angle during a turn at 50m/s, FCS authority is 10%*

By looking at the actual rotor pitch augmentations throughout the above bifurcation diagram, as in Figure 14, it can be seen that the lateral cyclic channel saturates first at $h_{1c} \approx$-0.270 and $h_{1c} \approx$-0.068, with the longitudinal SAS output saturating at $h_{1c} \approx$-0.335 and $h_{1c} \approx$-0.123. It is the saturation of the lateral cyclic that causes both points at which the bank angle starts to change more rapidly. The longitudinal saturation causes the onset on the small unstable sections of the branch.

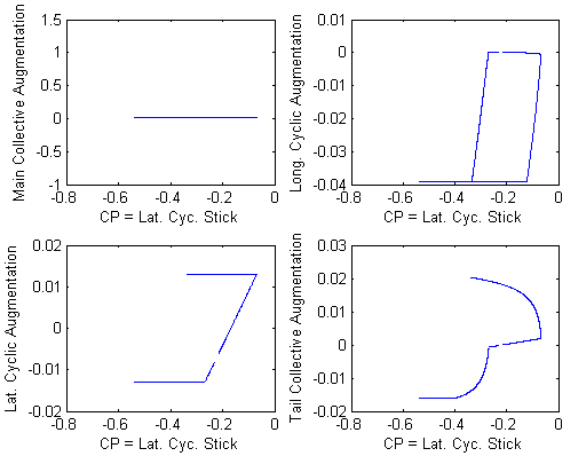

Figure 14. *Rotor augmentations from SAS with 10% authority during continuation of turning flight*

It would be desirable to increase the range over which the FCS is not saturated and delay the point at which the bank angle rate of change with lateral cyclic stick suddenly alters. Increasing the authority of the SAS can clearly do this. The authority is increased to 50%. Figure 15 shows a time history as the lateral cyclic is moved quasi statically to port. Again, then bank angle begins to increase faster at a cyclic stick position of about –0.68. This is a larger value than with only 10% SAS authority.

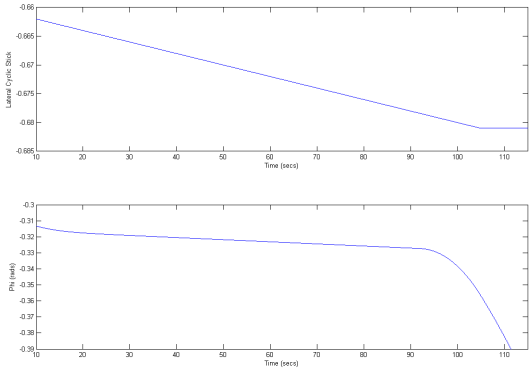

Figure 15. *Time History of turning flight as lateral cyclic stick is moved port, with 50% SAS authority*

The corresponding bifurcation diagrams with 50% SAS authority for all channels is shown in Figure 16. As expected, the points at which the lateral cyclic channel saturates have moved further apart, and are now at values of h_{1c}≈–0.68 and h_{1c}≈–0.325.

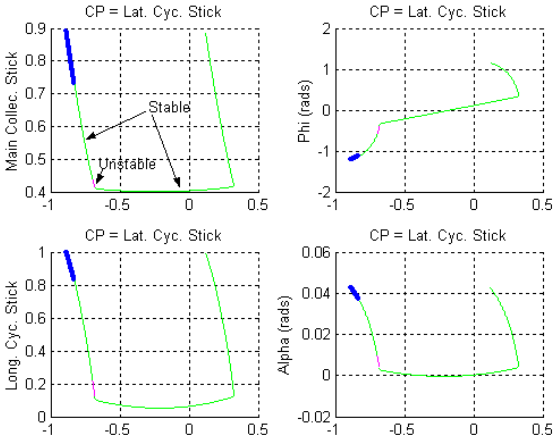

Figure 16. *Bifurcation diagram of bank angle during a turn at 50m/s, FCS authority is 50%*

The associated rotor pitch augmentation values during continuation are presented in Figure 17. The lateral cyclic saturation points are indeed at the values expected from the bifurcation diagram. No other control channel now saturates with their limits at 50% authority.

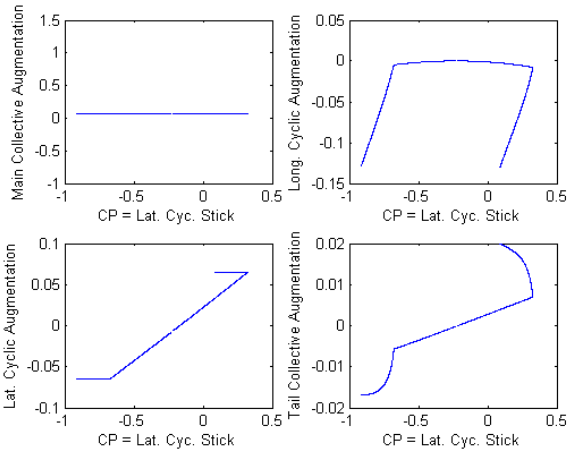

Figure 17. *Rotor augmentations from SAS with 50% authority during continuation of turning flight*

These results show the effect of increasing flight control system authority during turning manoeuvres.

5. Conclusions & Recommendations

This paper has demonstrated the use of continuation and bifurcation analysis when applied to both open loop and closed loop rotorcraft models, and shown the potential benefits when used in conjunction with simulation. Interesting phenomena have been presented, which have highlighted the high degree of asymmetry and the cross-coupled nature of rotorcraft.

The effect of two simple flight control systems has been investigated, and how bifurcation analysis may be used to evaluate their global

effect on the steady states of the helicopter, and examine the effect of variation of a controller gain. The handling qualities were found to be inadequate for the controller employed in this paper, but it is possible to integrate control law design methods into the continuation and bifurcation methodology, in order to ensure satisfactory handling qualities across a range of pilot inputs (Refs. 13-14).

Control system saturation has been shown to be a cause for Hopf points and the onset of instability, and the sudden change in state values with pilot controls. It has been shown that through increasing the control system authority, these effects can be changed.

Future work will address the issues of integration of controller design techniques into the continuation framework, and also the linking in of helicopter handling quality measures to ensure satisfactory response. All solutions to the system equations in this paper are equilibrium points. It is envisaged that periodic solutions to the equations will be solved for, and that these orbits can be used to help predict and understand more complex flight conditions and phenomena of rotorcraft. Along with this will be the increase in modelling fidelity brought by using a blade element representation of the main rotor, and so the rotorcraft will be a periodically forced system, will every solution being periodic with the rotational frequency of the rotor.

6. Acknowledgements

This activity has been conducted as part of a wider programme of QinetiQ-led flight control research, delivered to the MoD in accordance with the applied research requirements of DEC Air & Littoral Manoeuvre. The authors are therefore grateful to QinetiQ, Bedford and MoD for supporting the research, providing the Helilink generic light utility helicopter model and for sharing their expertise.

References

1. Sibilski, K., “Bifurcation Analysis of a Helicopter Non-Linear Dynamics,” 24th European rotorcraft Forum, Marseilles, France, Sept. 1998, Ref. Fm08

2. Sibilski, K., “Non-Linear Flight Mechanics of a Helicopter Analysis by Application of a Continuation Methods,” 25th European Rotorcraft Forum, Rome, Italy, Sept. 1999, Paper No. H4

3. Maradakis, G. S., “Fundamental Nonlinear Characteristics of Helicopter Flight Mechanics,” MPhil Thesis, Dept. of Applied Mathematics, Glasgow Caledonian University, Dec. 2000

4. Basset, P.-M. and Prasad, J. V. R., “Study of the Vortex Ring State using Bifurcation Theory,” Journal of the American Helicopter Society, Vol. 58, Montreal, Canada, Jun. 2000

5. Macmillen, F. B. J. and Thompson, J. M. T., “Bifurcation Analysis in the flight dynamics process? A view from the aircraft industry,” Philosophical Transactions: Mathematical and Engineering Sciences, Nonlinear flight dynamics of high-performance aircraft, Vol. 356, Royal Society of London, Series A, Oct. 1998, pp. 2321-2333

6. Goman, M. G., Zagainov, G. I. And Khramtsovsky, A. V., “Application of Bifurcation methods to Nonlinear Flight Dynamics Problems,” Prog. Aerospace Sci. Vol 33, pp. 539-586, 1997

7. Howitt, J., Strange, M. E. and Dudgeon, G. J. W., “An Investigation of the Impact of Flight Control System Saturation on Handling Qualities in Hover/Low Speed Manoeuvres,” American Helicopter Society 54th Annual Forum, Washington, D.C., May 1998

8. Whalley, M., Howitt, J. and Clift, S., “Optimization of Partial Authority Flight Control Systems for Hover/Low-Speed Manoeuvring in Degraded Visual Environments,” American Helicopter Society 55th Annual Forum, Montreal, Canada, May 1999

9. Seydel, R., “Practical bifurcation and stability analysis: from equilibrium to chaos,” 2nd Ed., New York, 1994

10. Lowenberg, M. H., “Bifurcation and Continuation Method,” Lecture Notes in Control and Information Sciences 283: Advanced Techniques for Clearance of Flight Control Laws, Springer, June 2002, pp89-106

11. Padfield, G. D., Helicopter Flight Dynamics, AIAA Education Series, 1995

12. Hughes, G., Manness, M. A. and Murray-Smith, D. J., “Eigenstructure Assignment Techniques for Handling Qualities in Helicopter Flight Control Law Design,” 16th European Rotorcraft Forum, Glasgow, Scotland, Sept. 1990, pp. III.10.2.1-13

13. Charles, G. A., di Bernado, M., Lowenberg, M. H., Stoten, D. P. and Wang, X. F., “Bifurcation Tailoring of Equilibria: a feedback control approach,” Journal of Latin American Applied Research, Special Theme issue Bifurcation Control: Methodologies and Applications, 31, 3, July 2001, pp199-210

14. Lowenberg, M. H. and Richardson, T. S., “Continuation Method Framework for Nonlinear Adaptive Controller Design,” Proceedings of AIAA Guidance Navigation & Control Conference, Montreal, Paper No. AIAA-2001-4100, Aug. 2001